Journal of Geophysical Research: Atmospheres

RESEARCH ARTICLE
10.1029/2018JD028637

**Key Points:**
- Initial sources for the polarity-reversal leader exhibit obvious height ascending and strong radiation power
- The polarity-reversal leader is initiated at the end of one decayed branch of the preceding leader
- Upward bipolar lightning flashes occurred at either a normal dipolar or an inverted dipolar charge structure

**Correspondence to:**
D. Shi,
w3914102@edu.gifu-u.ac.jp

**Citation:**
Shi, D., Wang, D., Wu, T., Thomas, R. J., Edens, H. E., Rison, W., Takagi, N., & Krehbiel, P. R. (2018). Leader polarity-reversal feature and charge structure of three upward bipolar lightning flashes. *Journal of Geophysical Research: Atmospheres*, *123*, 9430–9442. https://doi.org/10.1029/2018JD028637

Received 8 MAR 2018
Accepted 18 AUG 2018
Accepted article online 27 AUG 2018
Published online 12 SEP 2018



# Leader Polarity-Reversal Feature and Charge Structure of Three Upward Bipolar Lightning Flashes

**Dongdong Shi[1], Daohong Wang[1], Ting Wu[1], Ronald J. Thomas[2], Harald E. Edens[2], William Rison[2], Nobuyuki Takagi[1], and Paul R. Krehbiel[2]**

[1]Department of Electrical, Electronic and Computer Engineering, Gifu University, Gifu, Japan, [2]Langmuir Laboratory for Atmospheric Research, Geophysical Research Center, New Mexico Institute of Mining and Technology, Socorro, NM, USA

**Abstract** We have analyzed three upward bipolar lightning flashes (UBLFs) that occurred in Japanese winter thunderstorms. Leader polarity-reversal processes in three flashes share the same features. During the several tens of milliseconds (lightning A 56 ms, lightning B 21 ms, lightning C 67 ms) before the initiation of the polarity-reversal leader, one branch of the preceding leader in bipolar flashes was nearly decayed while other branches of the preceding leader were still in propagation. Then the polarity-reversal leader will be initiated at the end of the decayed branch of the preceding leader. Initial sources of the polarity-reversal leader are characterized by relatively strong very high frequency power (average value in lightning A, B, and C 24, 18, and 14 dBW) and obvious upward progression. Two of the three upward lightning (lightning A and B) occurred at a normal dipolar charge structure, while the remaining one (lightning C) occurred at an inverted dipolar charge structure. Based on the common features of the polarity-reversal leader and charge structure, we have proposed a scenario to interpret the process of upward bipolar lightning flashes.

## 1. Introduction

Bipolar lightning is so named because its electric current waveform exhibits polarity reversal, indicating both positive and negative charges are transferred to the ground, as first observed by McEachron (1939) and later observed by many others (e.g., Berger, 1978; Gorin & Shkilev, 1984). For a typical UBLF, since its positive and negative currents share the same channel as evident from many photos and videos (Berger & Vogelsanger, 1966; Wang & Takagi, 2008; Zhou et al., 2011), there must exist a polarity reversal in the leader discharges that caused the currents along the shared channel. An interesting question about UBLF is how the polarity reversal occurs. Wang and Takagi (2008) proposed a scenario for such leader polarity reversal and assumed that there must be two branches in the upward leader of bipolar lightning, with one branch having stopped progression while another branch being still in progression. The latter causes the electric field along the decayed branch reverse in direction. If the decayed branch is reactivated by the reversed electric field, a leader with reversed polarity will be generated. To test the scenario proposed by Wang and Takagi (2008), the leader progression inside cloud needs to be observed. Another interesting question about UBLF is what its charge structure looks like. Narita et al. (1989) explained that charge of both polarities followed the same channel to ground, but from the opposite-polarity charge regions separated horizontally in cloud. To test the charge structure suggested by Narita et al. (1989), the leader progression inside cloud also needs to be observed.

In the winter season of 2014, we have observed the leader progression of three UBLFs using lightning mapping array (LMA). For one of them, we had simultaneous current and electric field recording. For the remaining two events, we only had electric field recordings. In this paper, we will report on the leader polarity-reversal feature and charge structure of UBLF identified from their VHF source progressions in the cloud.

## 2. Observation and Data Description

We have been conducting a comprehensive observation campaign of lightning striking on the windmill and its lightning protection tower at Uchinanda, Ishikawa prefecture, Japan, since 2005 (Lu et al., 2009; Wang et al., 2008; Wang & Takagi, 2012; Wu et al., 2017). The windmill and the tower, both being erected on a small hill about 40 m above the sea level with a distance of 45 m, are 100 and 105 m in height, respectively. In order to further study the characteristics of upward lightning in Japanese winter thunderstorms, LMA with nine stations, forming an observation network of about 18 × 18 km$^2$ (Wu et al., 2017), was deployed for the first time near the coastal area of Japanese sea from 3 November 2014. The tower was around the center of the observation network, corresponding to (0,0) in Cartesian coordinate system. We restrict LMA sources with a chi-square value less than five in order to reduce noise.

Additional observation equipment includes a Rogowski coil and a field mill. Simultaneous current data with a sampling rate of 200 kHz is recorded by the Rogowski coil installed at the base of the tower. The electric field with atmospheric convention sign is recorded by the field mill with a distance of around 1.4 km from the windmill. Note that the field mill, with a time resolution of 50 ms, is not equipped with GPS timer and its synchronization with LMA can be done only manually with an uncertainty up to several hundred milliseconds.

Upward lightning can be subclassified into two types: self-initiated ones and other-triggered ones (Wang et al., 2008). If an upward lightning is triggered by some nearby lightning discharge activities, it will be defined as other-triggered upward lightning. If an upward lightning is initiated without any nearby preceding discharge activities, it will be named as self-initiated upward lightning. During the observation period, we recorded several self-initiated and other-triggered upward lightning flashes. Among them, three flashes are identified as UBLFs, one directly by current waveform and the remaining two by crosscheck of field mill data and LMA source locations.

## 3. Results

### 3.1. Upward Bipolar Lightning A

Upward bipolar lightning A occurred on 2 December 2014, hitting the lightning protection tower. Figure 1a shows altitude progression and initial stage current measured at the bottom of the tower. Figure 1b is the source radiation VHF power. Figures 1c and 1d are the vertical views along the direction of west-east and south-north, respectively. Figure 1e is the corresponding electric field. An upward positive leader (UPL), which transferred negative charge to the ground, was initiated from the tower at t1 and then propagated upward with an average speed of $10^4$ m/s. After propagating for about 21 ms, UPL reached up to a height of about 0.5 km at t2. At the height of 0.5 km, positive leader turned into horizontal direction as shown in Figures 1c and 1d and continued its progression. There was no obvious change in the corresponding electric current until t3. At t3, the current started to increase rapidly in its magnitude. At t4, the current reached to its negative peak of 2.4 kA, recovering to zero after about 62 ms. The total negative charge transferred to the ground during the negative current of initial stage was about $-40$ C. The transfer of the negative charge to the ground was also reflected in the corresponding electric field change from A to B shown in Figure 1e.

The current started to reverse its polarity at t7 and rose to its positive peak of 1.68 kA with 10–90% rising time of 2 ms at t8. In the LMA source altitude progression, correspondingly, an upward negative leader (UNL) was observed to propagate from the altitude of 1.5 to 2.8 km with vertical speed of $2.0 \times 10^5$ m/s. The corresponding source power of this upward leader, as seen in Figure 1b, was apparently larger than that produced by its previous discharges from t1 to t7 (average power: 24 versus $-1$ dBW). Both electric current and source power indicated that this upward leader was negative. This leader then turned into horizontal direction and transferred more positive charge to the ground. The duration of positive current was around 94 ms ranging from t7 to t9, and positive charge of 45 C was transferred to the ground. The negative change of electric field from B to C in Figure 1e also indicated that there was positive charge transferred to the ground. After t9, VHF sources rapidly fell to an altitude of 1 km and lasted for about 90 ms.

According to the distribution of source height and VHF power with average value of $-9.4$ dBW, these sources between t9 and t10 were produced by positive breakdown and negative charge was neutralized, which was also supported by the corresponding positive change from C to D in the electric field waveform. However, source locations between t9 and t10 did not share the same channel of preceding activities from t1 to t9. Therefore, current waveforms recorded at the tower base maintained positive polarity between t9 and t10.

Figure 2a indicates the three-dimensional (3-D) source distance from the tower, and Figures 2b–2d show the planar view of lightning sources at different stages. Around t5, the first source (shown by cyan square in Figure 2) that was near (3-D distance less than 1 km) the initial location of UNL indicated by pink triangle was apparently isolated from the preceding discharge channel at a horizontal distance of more than 2 km

10.1029/2018JD028637

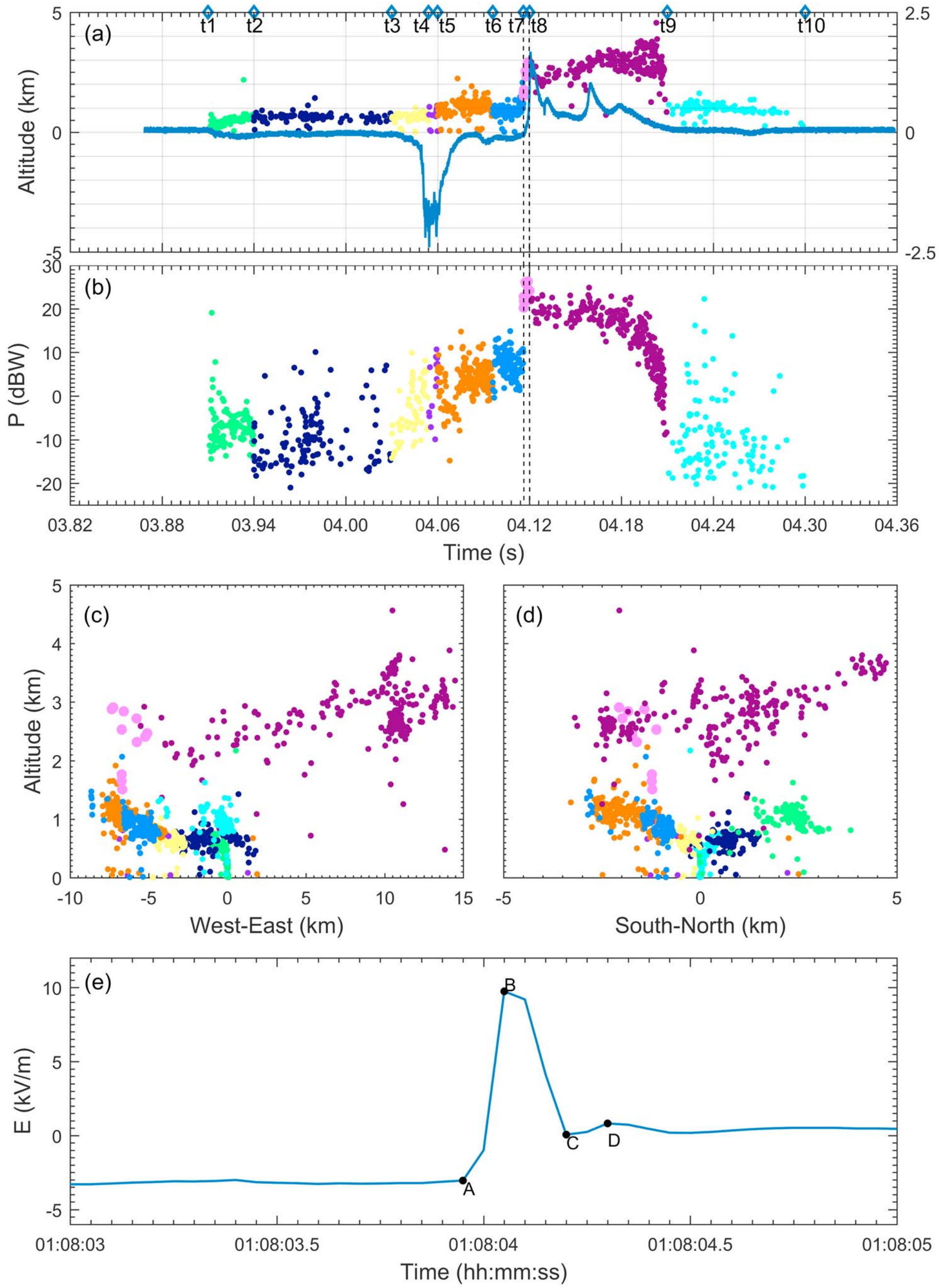


**Figure 1.** Three-dimensional source locations with recorded electric current and electric field of lightning A. (a) Current waveform superposed with source height versus time. (b) Power versus time. Figures 1a and 1b share the same time span at horizontal axis. (c) West-east vertical view. (d) South-north vertical view. (e) Ground electric field measured by the field mill. Figure 1e utilizes the independent time span at horizontal axis. The specific time represented by the marks in Figure 1a is listed as follows: t1 = UT01:08:03.910, t2 = UT01:08:03.940, t3 = UT01:08:04.030, t4 = UT01:08:04.054, t5 = UT01:08:04.060, t6 = UT01:08:04.096, t7 = UT01:08:04.116, t8 = UT01:08:04.120, t9 = UT01:08:04.210, and t10 = UT01:08:04.300.

as shown in Figure 2b. During the following 36 ms after t5, the leader propagated toward south-west direction as shown by red dots in Figure 2c. Between t6 and t7, the leader traversed back and reconnected to the disconnected path. Seen in Figure 2d, when the leader propagated backward, there were two obvious terminations marked by A and B. Apparently, blue dots and red dots are from two branches, namely, branch 1 and branch 2 in Figure 2d.

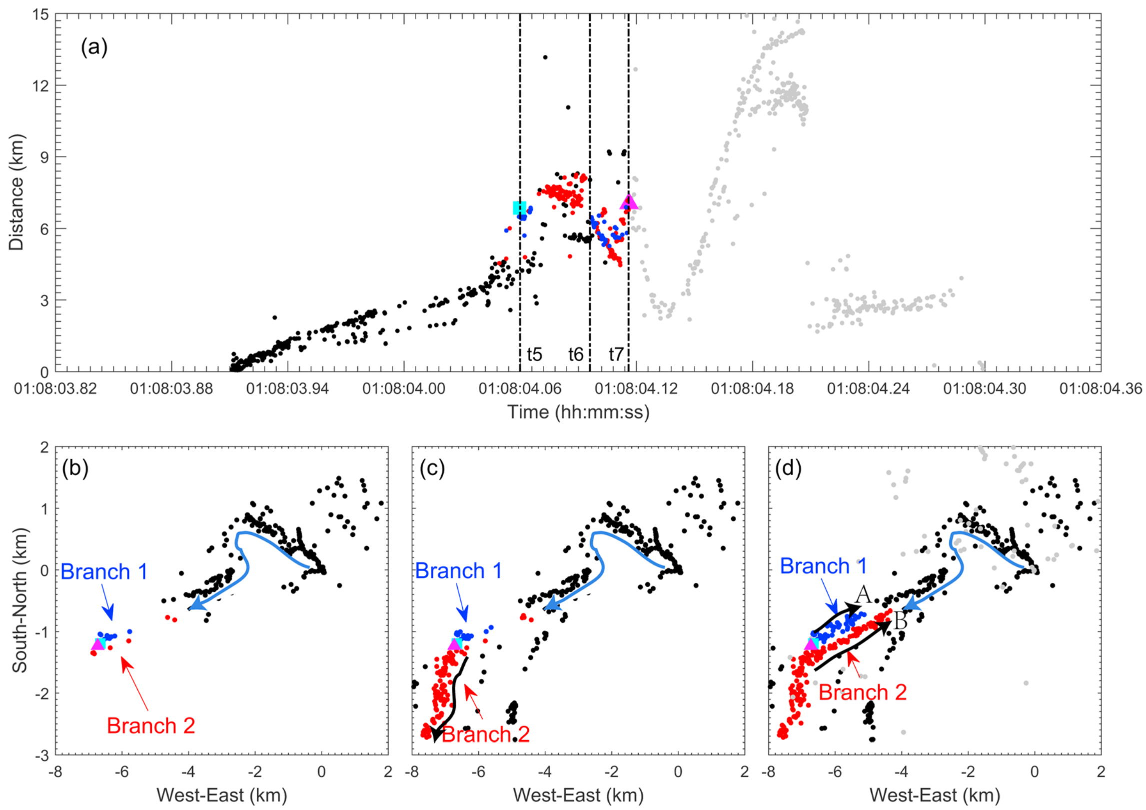


**Figure 2.** (a) Three-dimensional source distance from the tower with time, pink triangle representing the first source of UNL. Blue and red dots indicate sources of branch 1 and branch 2, respectively. Cyan square is the earliest source of branch 1 that is near the UNL initiation. Planar view of source distribution at different stages is shown in (b)–(d). (b) Source distribution before t5. (c) Source distribution before t6. (d) Source distribution before t7. Two obvious terminations are marked by A and B.

Initial sources of UNL occurred around the end of branch 1, about 56 ms (time interval from t5 to t7) after a few sources, blue dots in Figure 2b, happened near the same location. During the 56-ms period, branch 1 stopped propagating forward while branch 2 continued to develop toward south-west direction shown in Figure 2c. It seems that the process of polarity reversal has a strong relationship with branches of the preceding leader. Specific discussion will be given in section 4.

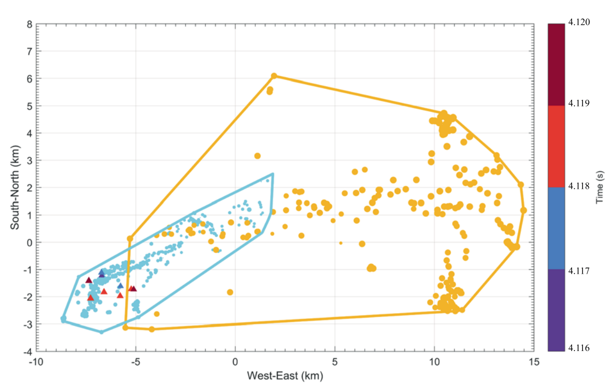


**Figure 3.** Planar view of charge structure for lightning A, orange and cyan circled lines representing positive and negative charge regions, respectively. Symbol size indicates source height. Triangles suggest initial sources of UNL with large VHF power, and their color represents sources' time with legend seen on the right side.

Planar view of charge structure for lightning A is given in Figure 3. Positive charge regions (PCR, inferred from t2 to t7) and negative charge regions (NCR, inferred from t8 to t9) are indicated by orange and cyan circled lines. Initial sources of UNL are indicated by triangles. The horizontal area covered by PCR and NCR is 134 and 24 $km^2$, respectively. PCR was above the NCR, forming a normal positive dipolar charge structure.

### 3.2. Upward Bipolar Lightning B

This lightning occurred on 14 November 2014, also hitting the protection tower. Its source locations, radiation power, and electric field recordings are shown in Figure 4. As seen in the source altitude progression (Figure 4a), prior to the initial upward leader, there were nearby preceding discharges as indicated by black points. Apparently, this lightning belonged to other-triggered type (Wang et al., 2008). Correspondingly, the electric field in Figure 4e, exhibiting a negative change before initiation of lightning B at the time of point A, supported the above inference as well.

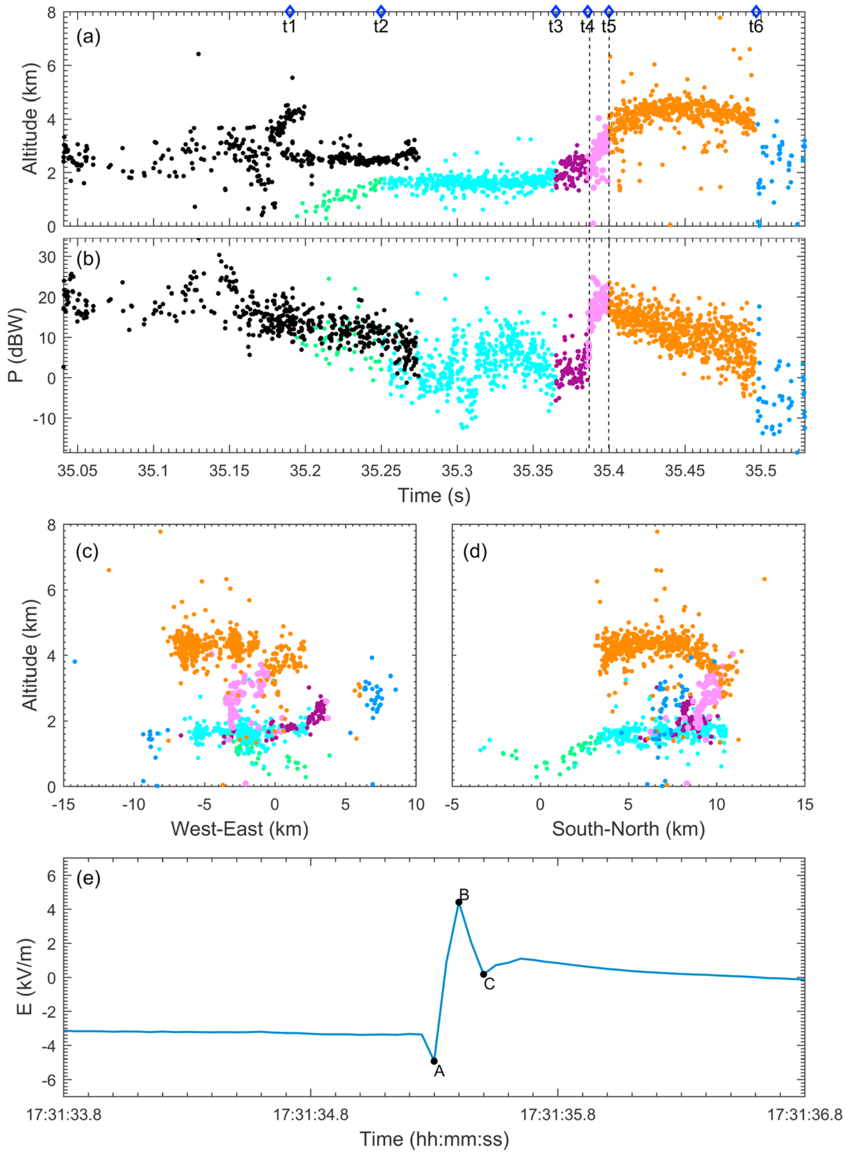


**Figure 4.** Three-dimensional source locations of lightning B. (a) Source height versus time. (b) Power versus time. Figures 4a and 4b share the same time span at horizontal axis. (c) West-east vertical view. (d) South-north vertical view. (e) Ground electric field measured by the field mill. Figure 4e utilizes the independent time span at horizontal axis. The specific time represented by the marks in Figure 4a is listed as follows: *t*1 = UT 17:31:35.190, *t*2 = UT 17:31:35.250, *t*3 = UT 17:31:35.365, t4 = UT 17:31:35.386, t5 = UT 17:31:35.400, and t6 = UT 17:31:35.497.

At t1, lightning B was initiated by UPL since electric field in Figure 4e first showed a positive change from point A to B, indicating that negative charge was transferred to the ground. Corresponding radiation power in Figure 4b showed a slight decreasing tendency during the stage of upward development. Sixty milliseconds after the initiation of lightning B, initial positive leader reached up to an altitude of 1.5 km with propagation speed of $10^4$ m/s and then turned into horizontal direction with slight height variation as shown in Figures 4c and 4d. As evident in Figures 4a and 4b, LMA sources between t4 and t5 exhibited a systematic altitude ascending from 2 to 3.5 km and VHF power increasing from 3 to 21 dBW, with an average value of 18 dBW. Meanwhile, electric field in Figure 4e showed a negative change from point B to C, indicating that positive charge was transferred to the ground. These features are similar to those observed in lightning A, and they combined lead us to judge that lightning B is an upward bipolar lightning flash.

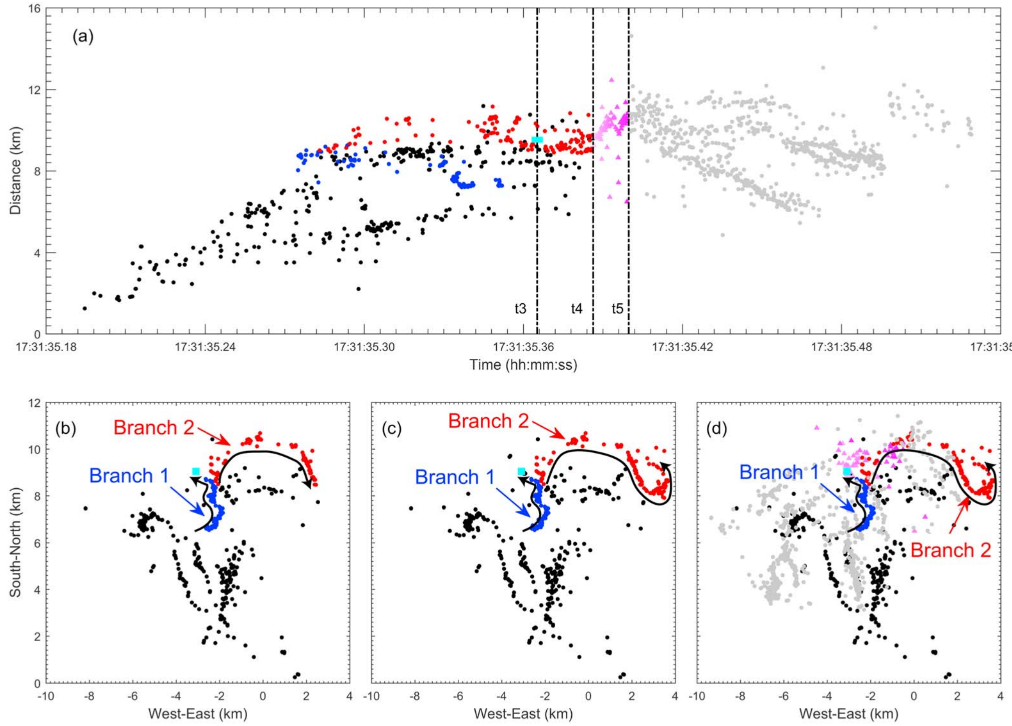


**Figure 5.** (a) Three-dimensional source distance from the tower with time. Planar view of source distribution at different stages is shown in (b)–(d). (b) Source distribution before t3. Cyan square is the earliest source that is near the initiation of UNL. Blue and red dots represent sources of branch 1 and branch 2. (c) Source distribution before t4. (d) Source distribution before t5. Triangles suggest initial sources of UNL, its transparency representing time.

Horizontal view of lightning B at different stages is given in Figure 5. Before t3, positive leader propagated with several branches, with two branches being denoted as branch 1 and branch 2 in Figure 5b. Seen from Figure 5b, the earliest source of branch 1 that was near (within 1 km in three dimensions) the initiation of UNL was marked by cyan square and happened at t3. After about 21 ms, namely, to the interval between t3 and t4, initial UNL sources (shown by triangles in Figure 5d) happened around the same position. These sources exhibited a 3-D speed of $1.2 \times 10^5$ m/s, which was estimated from the slope of source distance with time in Figure 5a. Similar to the phenomenon found in lightning A, during the 21-ms period, branch 2 continued to be in progression while branch 1 was nearly decayed and stopped further development, as indicated in Figure 5c. And then UNL was initiated at the end of the nearly decayed branch 1. It further implies that the occurrence of the polarity-reversal leader is related to the branches of the preceding leader discharges.

Planar view of charge structure for lightning B is shown in Figure 6. PCR (inferred from t2 to t4) overlapped NCR (inferred from t5 to t6). PCR and NCR showed almost the same wide extension (NCR versus PCR 55 versus 59 km$^2$), which was different from what lightning A showed (NCR versus PCR 24 versus 134 km$^2$). Since two UBLFs were both initiated with UPL, exhibiting a typical dipole charge structure, which contained a middle NCR and an upper PCR. However, charge layers inferred from lightning B was higher compared to that inferred from lightning A. For lightning A and B, middle NCR was at height of 0.8 and 1.7 km, respectively. Upper PCR was at height of 2.8 and 4.2 km, respectively.

### 3.3. Upward Bipolar Lightning C

Lightning C occurred on 14 November 2014, with a horizontal distance of more than 8 km from the tower. We also recognized this lightning as bipolar type because it was characterized with similar features of both LMA source locations and field mill data (shown in Figure 7) compared to what lightning A exhibited. However, since electric field in Figure 7e showed negative change from point A to B, lightning C was initiated with UNL, first transferring positive charge to the ground. Similar to lightning A, there was no obvious change

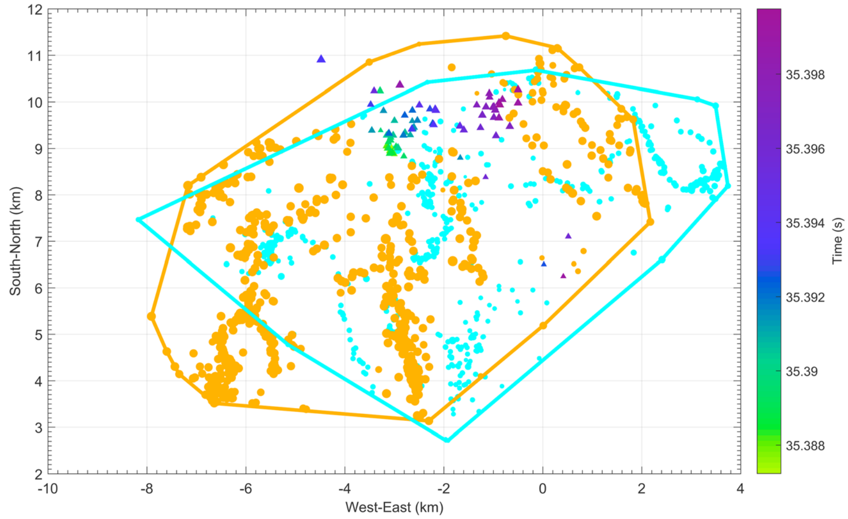


**Figure 6.** Planar view of charge structure for lightning B, orange and cyan circled lines representing positive and negative charge regions, respectively. Symbol size indicates source height. Triangles suggest initial sources of UNL and their color represents sources' time with legend seen on the right side.

in electric field before initiation of lightning C at the time of point A in Figure 7e and so we can classify lightning C into self-initiated type.

Lightning C was initiated at t1. In Figure 7a, initial UNL propagated from 0.8 to 2.5 km between t1 and t2, with propagation speed of $10^5$ m/s. During the process of obvious vertical development, the average VHF power of around 15 dBW in Figure 7b, relatively as strong as negative breakdown radiated among lightning A and B, was another demonstration for negative breakdown. Between t2 and t4, the leader turned into horizontal development in Figures 7c and 7d. Initial sources for polarity-reversal leader were between t4 and t5 since height transition from 3.5 to 5.0 km occurred and corresponding average vertical speed was $1.25 \times 10^5$ m/s. According to our observation, average VHF power of these initial sources of UPL was 14 dBW, apparently larger than positive breakdown radiated in lightning A ($-1$ dBW) and lightning B (4 dBW). However, since the preceding leader in lightning C was negative and VHF power of negative breakdown was naturally high (Rison et al., 1999), these initial sources of UPL in lightning C did not show rapid rise in VHF power as shown in Figure 7b, which was different from what lightning A and B exhibited in Figures 1b and 4b, respectively. After t5, recovery of electric field from point B to C in Figure 7e indicated that there was mainly negative charge transferred to the ground. In the whole process, source height exhibited two-layer distribution with center height of 2.5 and 5 km in Figures 7c and 7d, implying leaders' propagation in charge regions with different polarities.

For lightning C, we plotted the planar view as shown in Figure 8. After UNL was initiated, the leader propagated with several branches, denoted by branch 1, branch 2, and branch 3. Initial UPL sources were between t4 and t5. The earliest source that was close (3-D distance less than 1 km) to the origination of UPL happened at t3 and was marked by cyan square. During the 67-ms period, namely, to the interval between t3 and t4, branch 1 represented by blue dots has nearly stopped developing forward while branch 2 and branch 3 were still in progression, as shown in Figure 8c. The UPL was finally initiated around the end of the nearly decayed branch 1, very close to the position marked by cyan square in Figure 8. Here we need to point that since there were multiple concurrent branches of UNL in lightning C and LMA location results were discrete in space, the distinguish between branches for this lightning was not clear as in the cases of lightning A and lightning B. However, the phenomenon that UPL initiation in lightning C occurred close to the end of one branch of the preceding UNL was still seen in lightning C. It indicates again that polarity reversal has a strong relationship with branches of the preceding leader.

At the horizontal view, charge structure of lightning C is different from that of lightning A and B. Symbols in Figure 9 share the same meaning as those in Figures 3 and 6. Middle PCR (inferred from t2 to t4)

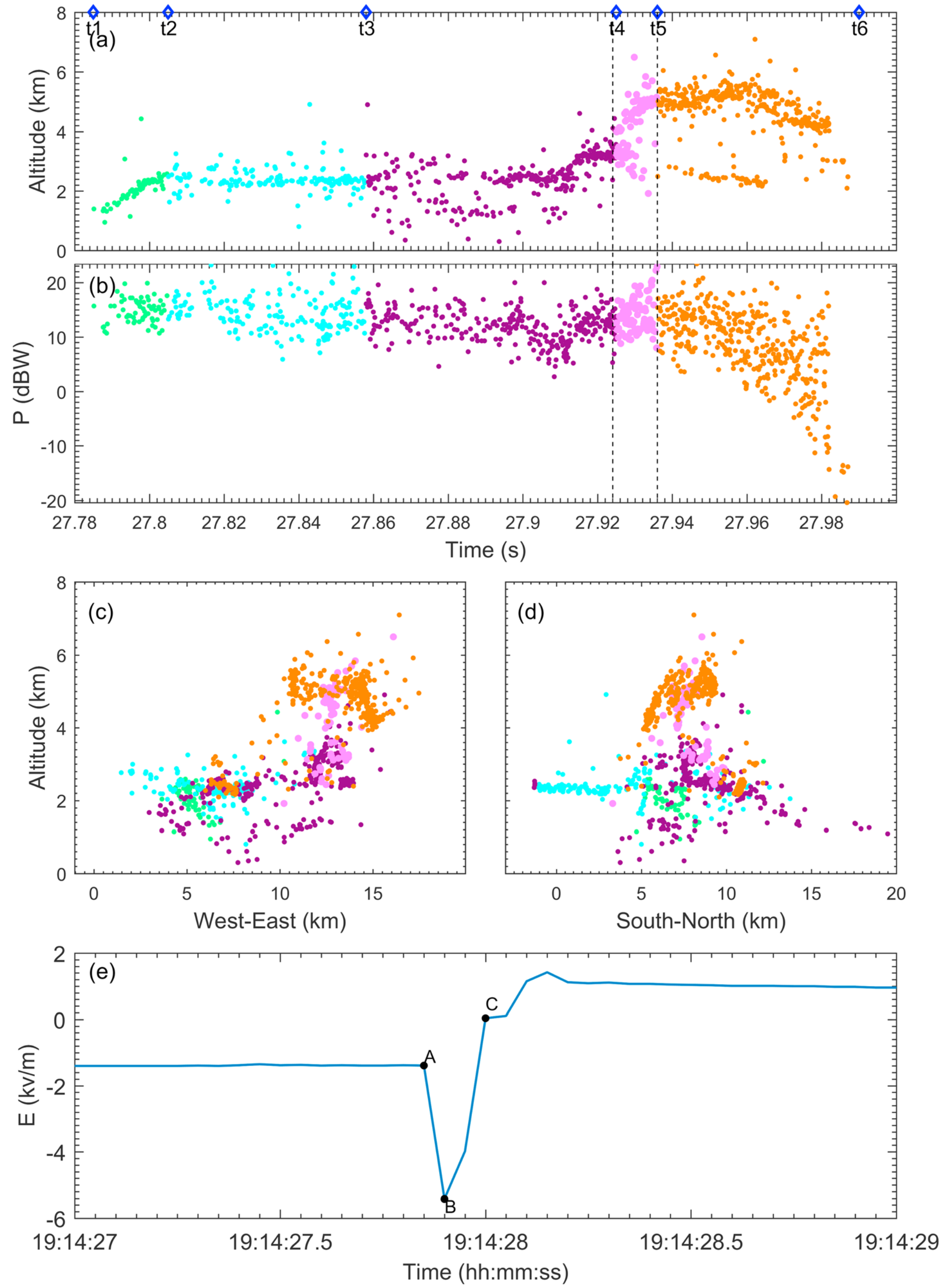


**Figure 7.** Three-dimensional source locations of lightning C. (a) Source height versus time. (b) Power versus time. Figures 7a and 7b share the same time span at horizontal axis. (c) West-east vertical view. (d) South-north vertical view. (e) Ground electric field measured by the field mill. Figure 7e utilizes the independent time span at horizontal axis. The specific time represented by the marks in Figure 7a is listed as follows: t1 = UT 19:14:27.785, t2 = UT 19:14:27.805, t3 = UT 19:14:27.858, t4 = UT 19:14:27.925, t5 = UT 19:14:27.936, and t6 = UT 19:14:27.990.

extended more widely than upper NCR (inferred from t5 to t6) did (PCR versus NCR 182 versus 62 $km^2$). Average height of PCR and NCR is 2.5 and 5 km. Furthermore, for both lightning A and lightning B, there existed a normal dipole charge structure with a middle NCR and an upper PCR. But lightning C exhibited an inverted-dipole charge structure with middle positively charging region and upper negatively charging region, consequently leading to the initiation of UNL followed by UPL. Hence, charge structure in thunderstorms has a significant influence on the polarity of initial upward leader.

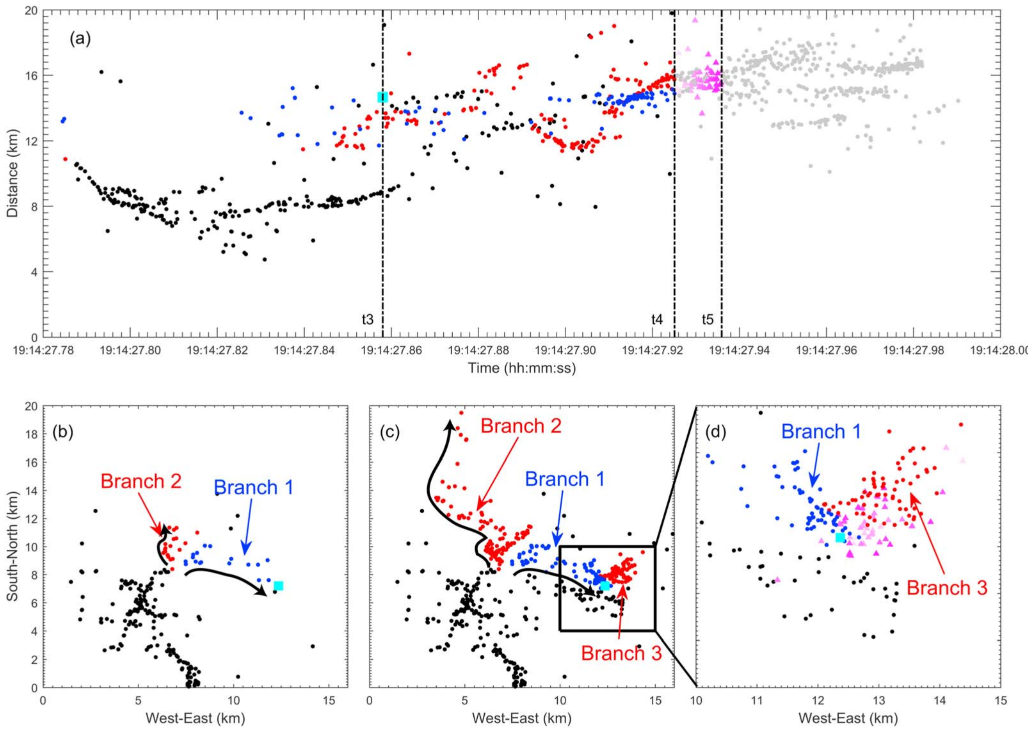


**Figure 8.** (a) Three-dimensional source distance from the tower with time. Planar view of source distribution at different stages is shown in (b)–(d). (b) Source distribution before t3. Cyan square is the earliest source that is near the initiation of UPL. Blue dots indicate sources of branch 1. Red dots represent sources of branch 2 and branch 3. (c) Source distribution before t4. (d) Source distribution before t5. The span of *y* axis is between 4 and 10 km.

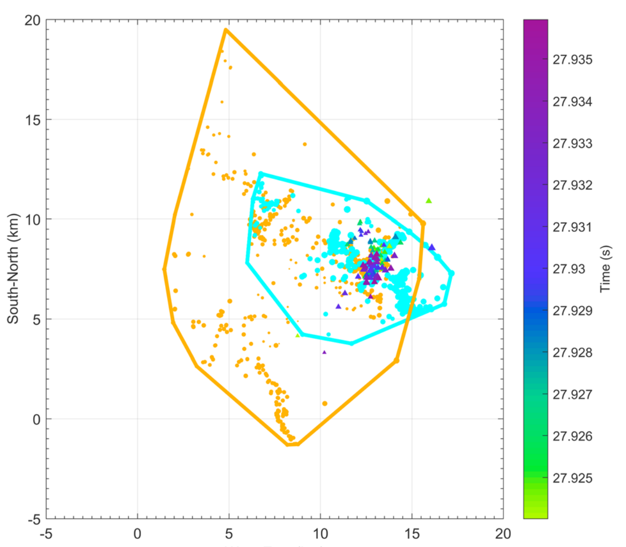


**Figure 9.** Planar view of charge structure for lightning C, orange and cyan circled lines representing positive and negative charge regions, respectively. Symbol size indicates source height. Triangles suggest initial sources of UPL and their color represents sources' time with legend seen on the right side.

## 4. Discussion

As seen from the planar view of three UBLFs (Figures 3, 6, and 9), for lightning A and lightning B, PCR overlaps the NCR, exhibiting a positive dipolar charge structure, while for lightning C, NCR is above the PCR, exhibiting an inverted dipolar charge structure. Apparently, UBLF does not necessarily need a unique charge structure, as opposed to that suggested by Narita et al. (1989). Besides, Japan winter thunderstorms are characterized with low cloud base, ranging from 200 to 800 m (Goto & Narita, 1992; Matsumoto et al., 2008). Consequently, charging height in Japan winter season, with center height of 2 and 4 km, is much lower than that in other regions' summer season (Krehbiel, 1986), resulting in relatively small vertical distance between two opposite-polarity charge layers. These factors combined may be conducive to the higher percentage of UBLF in Japanese winter thunderstorms.

As seen from the source locations in Figures 1a, 4a, and 7a, the two charge layers either in the dipolar or inverted-dipole structure were clearly bridged by an ascending leader that had opposite polarity to its previous upward leader. It is the bridge that channeled the charge of opposite polarity to the ground. Similar ascending leader serving as a bridge has been observed by Hill et al. (2013) in a bipolar lightning triggered with rocket-wire technique. As shown in Figures 2, 5, and 8, the ascending leader was formed at the end of a decayed branch. During the decay of the branch, discharges in other channels (or branches) are clearly in progress. All these observed facts basically support the scenario proposed by Wang and Takagi (2008) for the leader polarity reversal of UBLFs. With

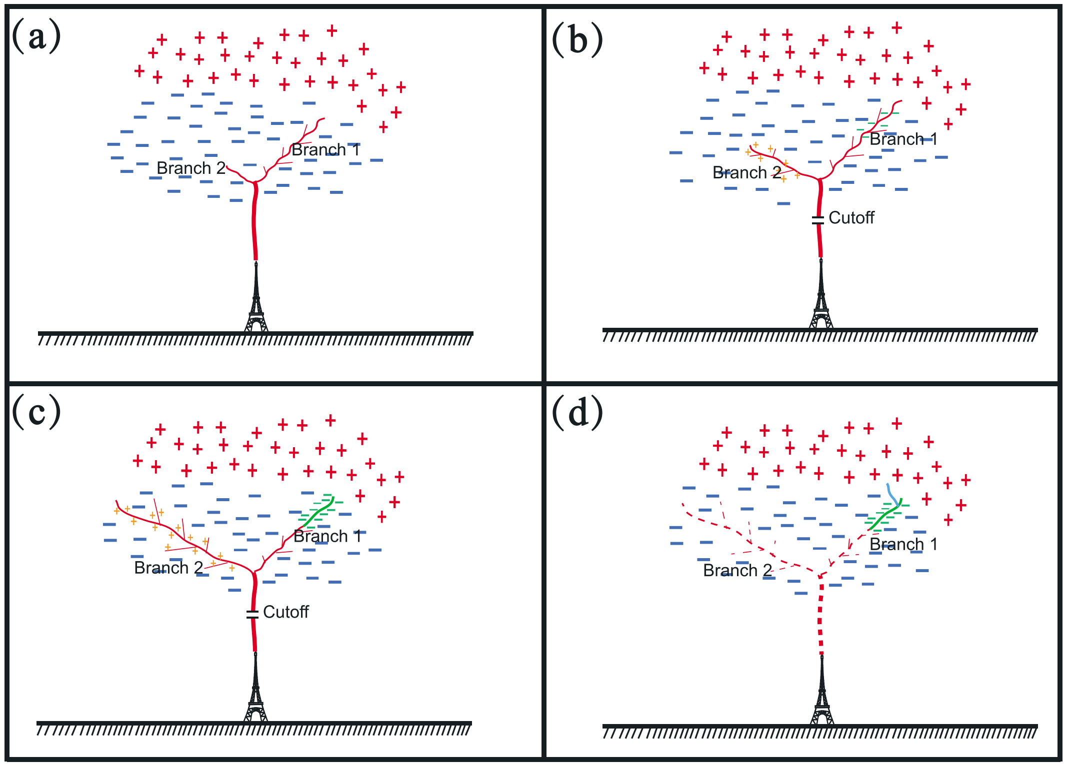


**Figure 10.** Process of leader polarity reversal of upward bipolar lightning flashes.

considering the charge structure and the detailed leader progression observed in the paper, Figure 10 presents an improved schematic to illustrate how a leader in reversed polarity is formed.

1. In Figure 10a, UPL propagating in NCR exhibits two branches, annotated as branch 1 and branch 2.
2. After branch 1 is nearly decayed, branch 2 still continues to be in progress. Because of occurrence of cutoff in the trunk channel, positive charge in the whole channel will be deposited along the forward direction of branch 2, but negative charge neutralized by branch 2 could not be transferred to the ground. On the contrary, since natural leader is bidirectional, those negative charge will be transferred in opposite direction along branch 2 and some of them are deposited at the end of branch 1 along the existed ionized channel, as indicated by Figure 10b.
3. With the further development of branch 2, more negative charge will be gathered at the end of branch 1, resulting in converting from the main positive to negative charging and then reversing the electric field, shown in Figure 10c.
4. In Figure 10d, UNL is initiated at the end of branch 1, thus the decayed branch 1 being reactivated by the reversed electric field. The trunk discharge channel is reconnected and positive charge is transferred to the ground, leading to polarity reversal in recorded current waveforms.

With this leader polarity reversal process embedded, we present a more complete progress of UBLF in Figure 11.

1. At time of t1, UPL is initiated on the tall object surrounded with corona charge.
2. At time of t2, UPL shows almost vertical propagation channel and attempts to access to the main charge region. At this time point, channel-base current is negative with low value due to relatively small amount of negative charge transferred to the ground.
3. At time of t3, positive leader travels through the center of NCR with slight height variation, which exhibits transition from vertical to nearly horizontal propagation. Meanwhile, negative charge is transferred to the ground continuously and electric current reaches up to negative peak.
4. At time of t4, with development of positive leader, some branches continue propagation motivated by ambient electric field while other branches stop developing, which validly reduces channel

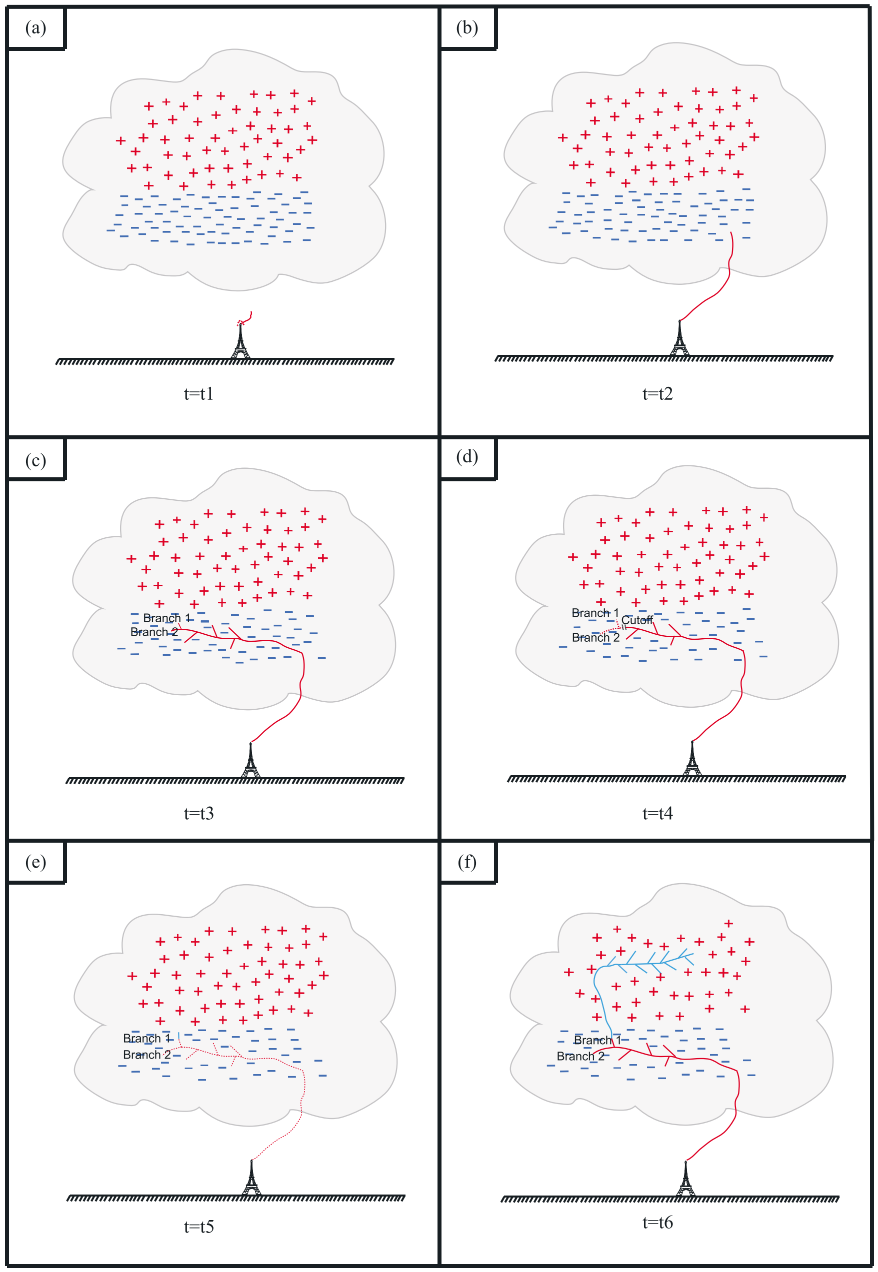


**Figure 11.** Schematic diagram for upward bipolar lightning flashes.

conductivity. According to our observation, we assume that cutoff occurs at somewhere of the trunk channel and consequently impedes the progress of lowering charge to the ground. Conversely, negative charge is deposited as much as possible at the end of already decayed branch 1.

5. At time of t5, deposited negative charge in the decayed branch 1, where positive charge was predominant, will produce a new electric field with reversal direction compared to original electric field. Model of inversing electric field and initiating UNL is depicted as Figure 10. Initial UNL shows obvious vertical propagation with relatively high VHF power. The trunk channel is reconnected since the initiation of UNL makes the channel well ionized again. Positive charge is transferred to the ground along the channel ionized by preceding positive breakdown, and the current polarity reversal takes place simultaneously.
6. At time of t6, negative leader with decreasing VHF power traverses through the center of PCR and transfers positive charge to the ground continuously before the channel conductivity decays.

Finally, we should point out that there is a type of bipolar lightning that is characterized by return strokes of opposite polarity (Saba et al., 2013; Saraiva et al., 2014; Tian et al., 2016; Zhu et al., 2016). For this type of bipolar lightning, either upward or downward, a recoil leader has been used to explain the polarity-reversal process by several authors (Saba et al., 2013; Saraiva et al., 2014; Tian et al., 2016; Zhu et al., 2016). So far, we have not observed such type of bipolar lightning with LMA. Whether the scenario shown in Figure 10 is applicable to this type of bipolar lightning is not known. In the future researches, this needs to be tested.

## 5. Conclusions

In this paper, we have reported three UBLFs observed in Japanese winter thunderstorms, one determined by current waveform and the other two co-confirmed through field mill and LMA source locations. Based on the above analysis, leader polarity-reversal process and charge structure that is conducive to the occurrence of UBLFs are characterized by the following common features:

1. A normal dipolar or an inverted dipolar charge structure in Japan is conducive to the occurrence of UBLF.
2. No matter of the initiation with UNL or UPL, LMA sources associated with polarity reversal exhibit height ascending with propagation speed of $10^5$ m/s in a short time. We infer that this phenomenon has a strong relationship with separation of charge regions and UBLF does traverse through two charge regions of different polarities.
3. VHF power of initial sources in the polarity-reversal leader (average value in lightning A, lightning B, and lightning C 24, 18, and 14 dBW) is significantly higher than that of subsequent sources with the same-polarity breakdown events. We suppose that the high VHF power attributes to breakdown in virgin air and strong electric field at the junction area between PCR and NCR.
4. Several tens of milliseconds (lightning A 56 ms, lightning B 21 ms, lightning C 67 ms) before the initiation of the polarity-reversal leader, the nearly decayed branch of the preceding leader has propagated to the position around which the subsequent polarity-reversal leader will be initiated. Model of inversing the electric field and the whole process for UBLF are proposed in section 4.

**Acknowledgments**

This research was supported by the Ministry of Education, Culture, Sports, Science, and Technology of Japan (grants 15H02597 and 16H04315). The data used for this paper were obtained during the winter campaign in 2014. The author would like to thank all the people who help carry out the related observation experiments. This work complies with the AGU data policy. Readers can get the data used in this paper from https://doi.org/10.5281/zenodo.1193452 or from the corresponding author (w3914102@edu.gifu-u.ac.jp).

## References

Berger, K. (1978). Blitzstrom-Parameter von Aufwartsblitzen. *Bulletin des Schweizerischen Elektrotechnischen Vereins*, *69*, 353–360.

Berger, K., & Vogelsanger, E. (1966). Photographische Blitzuntersuchungen der Jahre 1955–1965 auf dem Monte San Salvatore. *Bulletin des Schweizerischen Elektrotechnischen Vereins*, *57*, 599–620.

Gorin, B. N., & Shkilev, A. V. (1984). Measurements of lightning currents at the Ostankino tower. *Elektrichestvo*, *8*, 64–65.

Goto, Y., & Narita, K. (1992). Observations of winter lightning to an isolate tower. *Research Letters on Atmospheric Electricity*, *12*, 57–60.

Hill, J. D., Pilkey, J., Uman, M. A., Jordan, D. M., Rison, W., Krebhiel, P. R., et al. (2013). Correlated lightning mapping array and radar observations of the initial stages of three sequentially triggered Florida lightning discharges. *Journal of Geophysical Research: Atmospheres*, *118*, 8460–8481. https://doi.org/10.1002/jgrd.50660

Krehbiel, P. R. (1986). The electrical structure of thunderstorms. In E. P. Krider & R. G. Roble (Eds.), *The Earth's Electrical Environment* (pp. 90–113). Washington, DC: National Academy Press.

Lu, W., Wang, D., Zhang, Y., & Takagi, N. (2009). Two associated upward lightning flashes that produced opposite polarity electric field changes. *Geophysical Research Letters*, *36*, L05801. https://doi.org/10.1029/2008GL036598

Matsumoto, S., Ninomiya, K., & Akiyama, T. (2008). Cumulus activities in relation to the mesoscale convergence field. *Journal of the Meteorological Society of Japan*, *45*(4), 292–305. https://doi.org/10.2151/jmsj1965.45.4_292

McEachron, K. B. (1939). Lightning to the empire state building. *Journal of the Franklin Institute*, *227*(2), 149–217. https://doi.org/10.1016/s0016-0032(39)90397-2

Narita, K., Goto, Y., Komuro, H., & Sawada, S. (1989). Bipolar lightning in winter at Maki, japan. *Journal of Geophysical Research*, *94*(D11), 13,191–13,195. https://doi.org/10.1029/JD094id11p13191

Rison, W., Thomas, R. J., Krehbiel, P. R., Hamlin, T., & Harlin, J. (1999). A GPS-based three-dimensional lightning mapping system: Initial observations in central New Mexico. *Geophysical Research Letters*, *26*(23), 3573–3576. https://doi.org/10.1029/1999gl010856

Saba, M. M. F., Carina, S., Warner, T. A., Helsdon, J. H., Wolfgang, S., & Orville, R. E. (2013). Bipolar cloud-to-ground lightning flash observations. *Journal of Geophysical Research: Atmospheres*, *118*, 11,098–11,106. https://doi.org/10.1002/jgrd.50804

Saraiva, A. C. V., Campos, L. Z. S., Williams, E. R., Zepka, G. S., Alves, J., Pinto, O., et al. (2014). High speed video and electromagnetic analysis of two natural bipolar cloud-to-ground lightning flashes. *Journal of Geophysical Research: Atmospheres*, *119*, 6105–6127. https://doi.org/10.1002/2013JD020974

Tian, Y., Qie, X., Lu, G., Jiang, R., Wang, Z., Zhang, H., et al. (2016). Characteristics of a bipolar cloud-to-ground lightning flash containing a positive stroke followed by three negative strokes. *Atmospheric Research*, *176-177*, 222–230. https://doi.org/10.1016/j.atmosres.2016.02.023

Wang, D., & Takagi, N. (2008). Characteristics of upward bipolar lightning derived from Simultaneous recording of electric current and electric field change, Paper presented at the XXIX General Assembly, Int. Union of Radio Sci., Chicago, Ill.

Wang, D., & Takagi, N. (2012). Characteristics of winter lightning that occurred on a windmill and its lightning protection tower in Japan. *IEEJ Transactions on Power and Energy*, *132*(6), 568–572. https://doi.org/10.1541/ieejpes.132.568

Wang, D., Takagi, N., Watanabe, T., Sakurano, H., & Hashimoto, M. (2008). Observed characteristics of upward leaders that are initiated from a windmill and its lightning protection tower. *Geophysical Research Letters*, *35*, L02803. https://doi.org/10.1029/2007GL032136

Wu, T., Wang, D., Rison, W., Thomas, R. J., Edens, H. E., Takagi, N., & Krehbiel, P. R. (2017). Corona discharges from a windmill and its lightning protection tower in winter thunderstorms. *Journal of Geophysical Research: Atmospheres*, *122*, 4849–4865. https://doi.org/10.1002/2016JD025832

Zhou, H., Diendorfer, G., Thottappillil, R., Pichler, H., & Mair, M. (2011). Characteristics of upward bipolar lightning flashes observed at the Gaisberg tower. *Journal of Geophysical Research*, *116*, D13106. https://doi.org/10.1029/2011JD015634

Zhu, Y., Rakov, V. A., Tran, M. D., & Lu, W. (2016). A subsequent positive stroke developing in the channel of preceding negative stroke and containing bipolar continuing current. *Geophysical Research Letters*, *43*, 9948–9955. https://doi.org/10.1002/2016GL070475